# Domain switching in polycrystalline ferroelectric ceramics

J. Y. LI[1], R. C. ROGAN[2,3], E. ÜSTÜNDAG[3] AND K. BHATTACHARYA[2]*

[1]Department of Engineering Mechanics, University of Nebraska, Lincoln, Nebraska 68588-0526, USA
[2]Division of Engineering and Applied Science, California Institute of Technology, Pasadena, California 91125, USA
[3]Department of Materials Science and Engineering, Iowa State University, Ames, Iowa 50011-2300, USA
*e-mail: bhatta@caltech.edu

Published online: 18 September 2005; doi:10.1038/nmat1485

Ferroelectric ceramics are widely used as sensors and actuators for their electro-mechanical properties, and in electronic applications for their dielectric properties. Domain switching—the phenomenon wherein the ferroelectric material changes from one spontaneously polarized state to another under electrical or mechanical loads—is an important attribute of these materials. However, this is a complex collective process in commercially used polycrystalline ceramics that are agglomerations of a very large number of variously oriented grains. As the domains in one grain attempt to switch, they are constrained by the differently oriented neighbouring grains. Here we use a combined theoretical and experimental approach to establish a relation between crystallographic symmetry and the ability of a ferroelectric polycrystalline ceramic to switch. In particular, we show that equiaxed polycrystals of materials that are either tetragonal or rhombohedral cannot switch; yet polycrystals of materials where these two symmetries co-exist can in fact switch.

Ferroelectric perovskites such as lead titanate ($PbTiO_3$ or PT), lead zirconate ($PbZrO_3$ or PZ) and lead zirconate titanate ($Pb(Ti_xZr_{1-x})O_3$ or PZT) are widely used for their piezoelectric and dielectric properties[1–5]. These materials are nonpolar and cubic above the Curie temperature, but become spontaneously electrically polarized and mechanically distorted below this temperature. Owing to a reduction of symmetry at the Curie temperature, the spontaneous polarization can choose between several (crystallographic symmetry-related) directions. In fact, a typical crystal consists of intricate patterns of domains of different spontaneous polarization. The domain pattern may be changed or switched under sufficiently large electrical or mechanical loads. Domain switching is important in technological exploitation of ferroelectric ceramics during poling (a process wherein a large electric field is applied to a randomly oriented virgin ceramic to endow it with a remnant polarization through domain switching), in the so-called extrinsic component of electromechanical properties, and in electronic memory applications. Most ferroelectric materials are used in the form of ceramics, or polycrystals made of a very large number of variously oriented grains. Each grain contains several domains variously oriented among the crystallographically allowable directions of that grain. As the domains in one grain attempt to switch, they are constrained by the differently oriented neighbouring grains. Thus, domain switching in polycrystals is a highly correlated collective process.

There have been significant advances in understanding the (quantum-mechanical) origins of ferroelectricity using density functional theory[6–8], crystallographic and domain-wall structure using atomistic methods[9–12] and the evolution of domains using phase-field models[13–15]. Yet, these methods are too expensive to address domain switching in polycrystals, and this remains inadequately understood. This paper addresses it by developing a rigorous multiscale framework (Fig. 1) resulting in a coarse-grained theory validated by *in situ* observations. It shows that the polarizations and strains of the different variants in the single crystal should span a sufficiently large space to enable domain switching in a generic polycrystal. This establishes a relation between crystallographic symmetry and the ability of a polycrystal



©2005 Nature Publishing Group

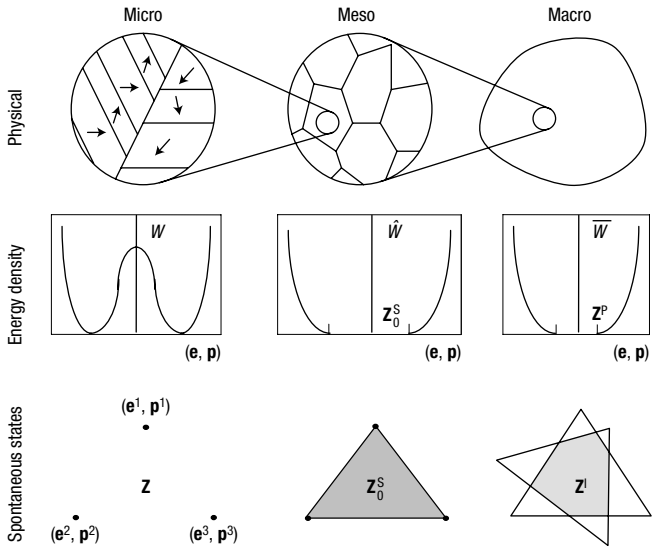


**Figure 1 The multiscale behaviour of a ferroelectric ceramic.** At the microscale, one has domains. This is described by an energy density $W$, which is zero on the set of spontaneous states Z and grows steeply away from it. At the mesoscale, one has grains with numerous domains. This is described by the effective energy density of a single crystal $\hat{W}$, which is zero on the effective set of spontaneous states of a single crystal $\mathbf{Z}_0^S$ consisting of compatible averages of points in Z. At the macroscale of the specimen, one has numerous grains with different domain structures. This is described by the effective energy density of a polycrystal $\overline{W}$, which is zero on the effective set of spontaneous states of a polycrystal $\mathbf{Z}^P$. The set $\mathbf{Z}^P$ can be estimated with $\mathbf{Z}^I$, which is simply the intersection of different copies of $\mathbf{Z}_0^S$ oriented suitably according to the crystallographic orientation of the grains.

to switch (Table 1). It also establishes that although polycrystals of a material that is either tetragonal or rhombohedral cannot switch, polycrystals of a material where these two symmetries co-exist can in fact switch. It provides quantitative estimates of the remnant strain, polarization and the domain distribution when subjected to electromechanical loading. It also identifies preferred textures for domain switching, and thus can guide current efforts of developing textured thin-film materials.

Of particular interest is the widely used PZT, a solid solution of PT and PZ. Titanium-rich PZT is $\langle 001\rangle_c$-polarized and tetragonal below the Curie temperature, whereas zirconium-rich PZT is $\langle 111\rangle_c$-polarized and rhombohedral below the Curie temperature. The exchange of stability takes place at the morphotropic phase boundary (MPB) around 48 at.% titanium: the material can exist in the $\langle 001\rangle_c$-polarized tetragonal, $\langle 111\rangle_c$-polarized rhombohedral and a variety of other lower symmetry states[4,16]. PZT is difficult to pole away from the MPB, but easy to pole at compositions close to the MPB[17–19]. This paper validates the long-standing intuition that the availability of multiple phases at the MPB makes it possible for the polarization to thread through the ceramic[20], and demonstrates the importance of strain compatibility that has not been fully realized before.

These issues are similar to the Taylor rule of plasticity that states that a crystal must have at least five slip systems for a polycrystal to be ductile[21] and the related result in shape-memory alloys[22]. However, the situation in ferroelectrics is more complicated with the electromechanical coupling, and the results are more nuanced. Further, the ferroelectric PZT system allows an experimental investigation spanning different symmetries in a single system. Finally, the results presented here are relevant to ferromagnetic shape-memory alloys such as $Ni_2MnGa$ (ref. 23).

## THEORY

A coarse-grained theory that describes the overall behaviour of a ceramic shown in Fig. 1 containing numerous grains, each containing numerous domains, has been derived starting from a Devonshire–Ginzburg–Landau (DGL)-type theory. Further details have been provided online as Supplementary Information.

At the smallest length scale (micro), a ferroelectric material is described by a DGL-type theory with an energy density $W(\mathbf{e},\mathbf{p})$ that depends on the state variables, strain $\mathbf{e}$ and polarization $\mathbf{p}$. The ferroelectric material may be spontaneously polarized and strained in one of $K$ crystallographically equivalent variants. Let $\mathbf{e}^{(i)}$ denote the spontaneous strain and $\mathbf{p}^{(i)}$ the spontaneous polarization of the $i$th variant ($i=1,\ldots,K$). $W$ has its minima (zero without loss of generality) on the set of spontaneous states $\mathbf{Z}=\cup_{i=1}^{K}\{(\mathbf{e}^{(i)},\mathbf{p}^{(i)})\}$ and grows quickly away from it.

The multiwell structure of $W$ leads to the formation of domain patterns. The overall behaviour over the scale of a domain pattern (meso) is described by the effective energy density of a single crystal $\hat{W}(\mathbf{e},\mathbf{p})$ defined in equation (4) of the Supplementary Information. It implicitly accounts for the domains. It has its minima on the set of effective spontaneous states of the single crystal $\mathbf{Z}_0^S$ that contains the average spontaneous strains and polarizations of domain patterns. The domain patterns cannot be arbitrary; instead they have to be compatible. Two variants $j$ and $k$ can form a domain pattern if an only if they satisfy two compatibility conditions[24],

$$\mathbf{e}^{(j)}-\mathbf{e}^{(k)}=\frac{1}{2}(\mathbf{a}\otimes\mathbf{n}+\mathbf{n}\otimes\mathbf{a}),\qquad(\mathbf{p}^{(j)}-\mathbf{p}^{(k)})\cdot\mathbf{n}=0,\qquad(1)$$

where $\mathbf{n}$ is the normal to the interface. The first is the mechanical compatibility condition that ensures the mechanical integrity of the interface, and the second is the electrical compatibility condition that ensures an uncharged interface. It is possible to classify domain walls by studying the solutions of these equations[24]. If equation (1) holds, the two variants can form a laminate pattern with volume fraction $\lambda$ and average spontaneous strain and polarization,

$$\hat{\mathbf{e}}=\lambda\mathbf{e}^{(j)}+(1-\lambda)\mathbf{e}^{(k)},\qquad\hat{\mathbf{p}}=\lambda\mathbf{p}^{(j)}+(1-\lambda)\mathbf{p}^{(k)}.$$

As the number of variants increases, the domain patterns become more complicated and it is important to generalize equation (1). For example, if we have four variants $i$, $j$, $k$ and $l$, they can form a herring-bone (double laminate) pattern with $i$, $j$ on one side and $k$, $l$ on the other if and only if they satisfy

$$\mathbf{e}^{(i)}-\mathbf{e}^{(j)}=\frac{1}{2}(\mathbf{a}_1\otimes\mathbf{n}_1+\mathbf{n}_1\otimes\mathbf{a}_1),\qquad(\mathbf{p}^{(i)}-\mathbf{p}^{(j)})\cdot\mathbf{n}_1=0;$$

$$\mathbf{e}^{(k)}-\mathbf{e}^{(l)}=\frac{1}{2}(\mathbf{a}_2\otimes\mathbf{n}_2+\mathbf{n}_2\otimes\mathbf{a}_2),\qquad(\mathbf{p}^{(k)}-\mathbf{p}^{(l)})\cdot\mathbf{n}_2=0;$$

$$\left(\lambda_1\mathbf{e}^{(i)}+(1-\lambda_1)\mathbf{e}^{(j)}\right)-\left(\lambda_2\mathbf{e}^{(k)}+(1-\lambda_2)\mathbf{e}^{(l)}\right)=\frac{1}{2}(\mathbf{a}_3\otimes\mathbf{n}_3+\mathbf{n}_3\otimes\mathbf{a}_3),$$

$$\left(\left(\lambda_1\mathbf{p}^{(i)}+(1-\lambda_1)\mathbf{p}^{(j)}\right)-\left(\lambda_2\mathbf{p}^{(k)}+(1-\lambda_2)\mathbf{p}^{(l)}\right)\right)\cdot\mathbf{n}_3=0.$$

Note that the compatibility across the mid-plane of the herring-bone is imposed in an average manner. Variant $i$ does not have to be compatible with either variants $k$ or $l$; instead, an appropriate average of variants $i,j$ has to be compatible with an average of variants $k,l$. This means that the pattern can have small mismatches on the scale of an individual domain, but is still compatible on a larger scale that is much smaller than the entire pattern. The physical basis for the formation of such patterns and a sophisticated mathematical framework to describe them has been developed[24–26]. In any case, computing the set $\mathbf{Z}_0^S$ of possible effective spontaneous polarization and strains is a significant challenge. Yet, we have



©2005 Nature Publishing Group

**Table 1 Summary of results. The ability of domains to switch in ferroelectric polycrystals depends critically on the crystallographic symmetry of the ferroelectric phase. The results in this table assume that the high-temperature nonpolar phase is cubic.**

| Symmetry of ferroelectric phase | Non-180° domain switching in ceramics? | Strain through non-180° domain switching in ceramics? | Ratio of ceramic to single-crystal remnant polarization | Requisite texture for non-180° domain switching |
|---|---|---|---|---|
| Tetragonal | No | No | $1/3$ | $\langle 001\rangle_c$ |
| Rhombohedral | Yes | No | $1/\sqrt{2}$ | $\langle 111\rangle_c$ |
| Tetragonal–rhombohedral co-existence | Yes | Yes | $\sim 1$ | Arbitrary |
| Monoclinic | Yes | Yes | $\sim 1$ | Arbitrary |

the following result[25,27]: Suppose the ferroelectric material has $K$ variants, and each pair of variants satisfies equation (1). Then, $\mathbf{Z}_0^{\mathrm{S}}$ is given by all possible averages of spontaneous strains and polarizations:

$$\mathbf{Z}_0^{\mathrm{S}} = \left\{ (\mathbf{e},\mathbf{p}) : \mathbf{e} = \sum_{i=1}^{K} \lambda_i \mathbf{e}^{(i)},\ \mathbf{p} = \sum_{i=1}^{K} \lambda_i \mathbf{p}^{(i)},\ \lambda_i \geq 0,\ \sum_{i=1}^{K} \lambda_i = 1 \right\}. \quad (2)$$

In other words, if each pair of variants is compatible, then compatibility poses no restriction, and it is possible to find compatible domain patterns for any arbitrary average. This is shown schematically in Fig. 1.

A polycrystal is a collection of perfectly bonded single crystals with a large number of distinct orientations. Let $\mathbf{R}(\mathbf{x})$ denote the orientation of the grain at $\mathbf{x}$; that is, let $\mathbf{R}(\mathbf{x})$ be the rotation matrix that takes the laboratory frame to the crystal frame of the grain at $\mathbf{x}$. The effective energy density of the grain at $\mathbf{x}$ is $\hat{W}(\mathbf{R}(\mathbf{x})\mathbf{e}\mathbf{R}^{\mathrm{T}}(\mathbf{x}), \mathbf{R}(\mathbf{x})\mathbf{p})$, and the sets $\mathbf{Z}(\mathbf{x})$ and $\mathbf{Z}^{\mathrm{S}}(\mathbf{x})$ corresponding to this grain are given by a suitable reorientation of $\mathbf{Z}$ and $\mathbf{Z}_0^{\mathrm{S}}$:

$$\begin{aligned} \mathbf{Z}(\mathbf{x}) &= \bigcup_{i=1}^{K} \left\{ (\mathbf{R}(\mathbf{x})\mathbf{e}^{(i)}\mathbf{R}^{\mathrm{T}}(\mathbf{x}), \mathbf{R}(\mathbf{x})\mathbf{p}^{(i)}) \right\} \\ &= \left\{ \mathbf{R}(\mathbf{x})\mathbf{e}\mathbf{R}^{\mathrm{T}}(\mathbf{x}), \mathbf{R}(\mathbf{x})\mathbf{p} : (\mathbf{e},\mathbf{p}) \in \mathbf{Z} \right\}, \\ \mathbf{Z}^{\mathrm{S}}(\mathbf{x}) &= \left\{ \mathbf{R}(\mathbf{x})\mathbf{e}\mathbf{R}^{\mathrm{T}}(\mathbf{x}), \mathbf{R}(\mathbf{x})\mathbf{p} : (\mathbf{e},\mathbf{p}) \in \mathbf{Z}_0^{\mathrm{S}} \right\}. \end{aligned}$$

The properties of the polycrystal are determined by the collective behaviour of a large number of grains. Therefore, its behaviour is described by the effective energy density of the polycrystal $\overline{W}(\mathbf{e},\mathbf{p})$ defined in equation (9) of the Supplementary Information that implicitly accounts for all grains and domains. This energy density has its minima on the set of effective spontaneous states of the polycrystal $\mathbf{Z}^{\mathrm{P}}$. To elaborate on this concept, note that one has a large number of grains and the domain pattern can change from one part of a grain to another. To capture this, we introduce a mesoscale strain and polarization field that averages over the domain patterns, but still varies at the scale of the grains. We say that such a strain and polarization field can be accommodated by the polycrystal if it is compatible and if it belongs at each point $\mathbf{x}$ to the corresponding set $\mathbf{Z}^{\mathrm{S}}(\mathbf{x})$. Physically, the domain patterns and the resulting locally averaged polarization and strain have to be compatible at the scale of the grains both within each grain and across the grain boundary; however, one can have incompatibilities at the scale of individual domains. $\mathbf{Z}^{\mathrm{P}}$ is the set of all strains and polarizations that can be obtained as macroscopic averages of such accommodated mesoscale strain and polarization fields. Therefore, $\mathbf{Z}^{\mathrm{P}}$ implicitly accounts for both the intergranular constraints and the cooperative effects of multiple grains and quantifies the range of polarizations and strains that one can expect through domain switching.

It is difficult to evaluate $\overline{W}$ and, thus, the set $\mathbf{Z}^{\mathrm{P}}$ explicitly, but they can be characterized using bounds. An upper bound on the energy $\overline{W}$ and an inner bound on $\mathbf{Z}^{\mathrm{P}}$ following the Hashin–Strikhman variational principle is particularly useful, and leads to a simple algebraic formula:

$$\begin{aligned} \mathbf{Z}^{\mathrm{P}} \supseteq \mathbf{Z}^{I} &= \bigcap_{\mathbf{x}\in\Omega} \mathbf{Z}^{\mathrm{S}}(\mathbf{x}) \\ &= \left\{ (\mathbf{e},\mathbf{p}) : \left(\mathbf{R}(\mathbf{x})\mathbf{e}\mathbf{R}^{\mathrm{T}}(\mathbf{x}), \mathbf{R}(\mathbf{x})\mathbf{p}\right) \in \mathbf{Z}^{\mathrm{S}}(\mathbf{x}) \forall \mathbf{x} \in \Omega \right\}. \quad (3) \end{aligned}$$

The set $\mathbf{Z}^{\mathrm{I}}$ has the straightforward geometric interpretation shown in Fig. 1: it is the intersection of the sets $\mathbf{Z}^{\mathrm{S}}(\mathbf{x})$ of all grains. So it contains the common effective strains and polarizations of all grains. This simple bound is a surprisingly good indicator of the actual behaviour of the material.

## RESULTS

### SINGLE-PHASE TETRAGONAL MATERIALS

A material such as barium titanate (BT), PT or titanium-rich PZT (for example 60% Ti) is cubic above the Curie temperature and spontaneously polarized and elongated along one of the six $\langle 001\rangle_c$ directions below that temperature. There are six variants with spontaneous strains and polarizations of the form

$$\mathbf{e}^{(1)} = \begin{pmatrix} \beta & & \\ & \alpha & \\ & & \alpha \end{pmatrix}, \quad \mathbf{p}^{(1)} = p^t \begin{pmatrix} 1 \\ 0 \\ 0 \end{pmatrix}, \quad (4)$$

and their symmetric permutations. Each pair of variants is compatible and one can use equation (2) to calculate $\mathbf{Z}_0^{\mathrm{S}}$. Carrying out the algebra, the effective spontaneous strains of single crystals are found to have fixed trace $(2\alpha+\beta)$ and zero off-diagonal elements and the effective spontaneous polarizations are contained in a parallopiped $|p_i| \leq ((\alpha - e_{ii})/(\alpha-\beta))p^t$. So, these strains lie in a two-dimensional subspace of the five-dimensional linear space of deviatoric (shear-like) strains, but the polarizations span the entire three-dimensional linear space of polarizations. Substituting $\mathbf{Z}_0^{\mathrm{S}}$ in equation (3) to calculate $\mathbf{Z}^{\mathrm{I}}$ leads to two conclusions. First, the set $\mathbf{Z}^{\mathrm{I}}$ contains only a single point in strain space unless the orientations of the grains are limited to having a common $\langle 001\rangle_c$ axis. In other words, unless the polycrystal has a $\langle 001\rangle_c$ texture, the intergranular mechanical constraints prevent any macroscopic spontaneous strain. If the polycrystal has $\langle 001\rangle_c$ texture, the intergranular mechanical constraints allow uniaxial strain along the $\langle 001\rangle_c$ axis. Second, the set $\mathbf{Z}^{\mathrm{I}}$ contains at least a small ball in the polarization space. Therefore a polycrystal can have non-zero effective spontaneous polarization irrespective of texture. For an equiaxed (random) polycrystal, the effective spontaneous polarization is equal to $p^t/3$. These calculations also show that given any effective spontaneous strain and polarization in the set $\mathbf{Z}^{\mathrm{S}}$, there is a unique proportion of the different variants that can attain it. Thus, there is a one-to-one correlation between volume fractions and macroscopic properties.

It follows that an equiaxed tetragonal polycrystal will show no 90° domain switching, no macroscopic strains through domain



©2005 Nature Publishing Group

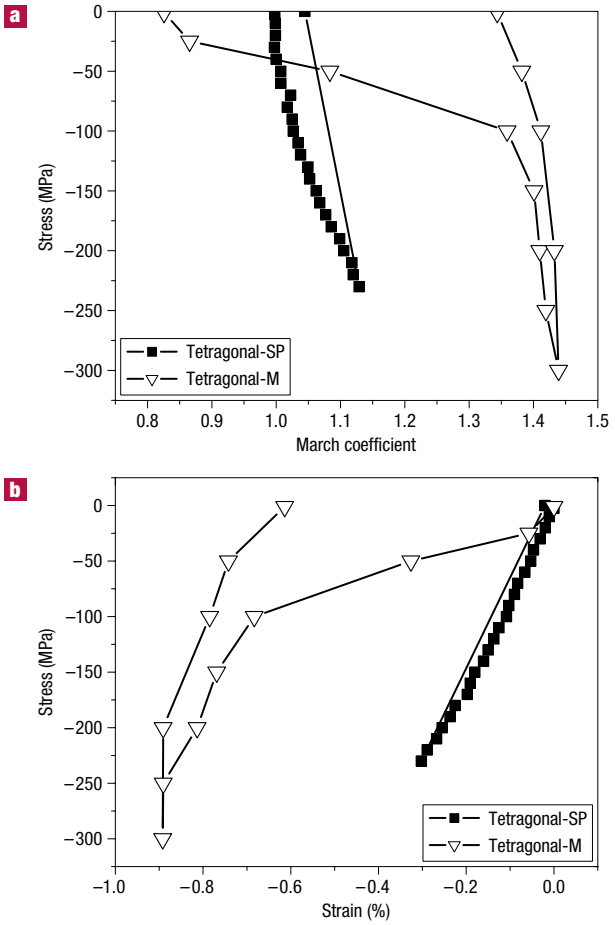


**Figure 2 The evolution under uniaxial compressive stress of the tetragonal domains and the associated strain for two different specimens of PZT, 40/60 (tetragonal-SP) and 49/51 (tetragonal-M), measured *in situ* using neutron diffraction. a**,**b**, March coefficient (**a**) and longitudinal lattice strains (**b**) referenced to the zero-load state. The 40/60 specimen that contains only tetragonal domains shows no 90° domain switching and only linear strain, whereas the morphotropic 49/51 specimen that contains both tetragonal and rhombohedral domains shows significant 90° domain switching and nonlinear strain. Fitting errors are of the order of the data point symbol size and have been omitted for clarity.

switching and only limited poling through 180° domain switching with macroscopic spontaneous polarization limited to a third of the single-crystal value. A $\langle 001 \rangle_c$ fibre-texture is necessary for 90° domain switching.

The first two predictions are consistent with the results of neutron diffraction experiments on titanium-rich (60% Ti) PZT shown in Fig. 2 as tetragonal-SP. Details of the experiment and the representation of the results using a March coefficient are given in the Methods section. Briefly, a March coefficient of one indicates random or equiaxed texture, values less than unity indicate alignment of the polarizations along a fibre direction, and values greater than unity indicate distribution of the polarizations normal to a fibre direction. Figure 2a shows that the March coefficient of the specimen is close to one before, during and after loading indicating equiaxed texture and no 90° switching during either electrical poling or mechanical loading. Figure 2b shows that the elastic strains are essentially linear and show no permanent change on unloading. The third prediction clears up a long-standing open issue. The single-crystal spontaneous polarization value of $BaTiO_3$ is 26 μC cm$^{-2}$ and the polycrystal value is 8 μC cm$^{-2}$ in agreement with the current prediction of 8.67 μC cm$^{-2}$ (and in contrast to the classical prediction of 21.6 μC cm$^{-2}$, which does not take the compatibility between the grains into account)[4,28]. In PZT[19], the ceramic spontaneous polarization at 48%-Zr is 17 μC cm$^{-2}$, and this is about a third of the MPB value of 48 μC cm$^{-2}$ consistent with the prediction (we show below that the MPB ceramic and single-crystal values are comparable). The prediction is also consistent with the observed sharp drop of spontaneous polarization of PZT for Zr content below MPB[19].

## SINGLE-PHASE RHOMBOHEDRAL MATERIALS

A material such as Zr-rich PZT (for example, 60% Zr) or lead-zirconate-niobate/lead-titanate (PZN–PT) is cubic above the Curie temperature and spontaneously polarized and elongated along one of the eight $\langle 111 \rangle_c$ directions below this temperature. Thus, one has eight variants with spontaneous strains and polarizations of the form

$$\mathbf{e}^{(1)} = \begin{pmatrix} \eta & \delta & \delta \\ \delta & \eta & \delta \\ \delta & \delta & \eta \end{pmatrix}, \quad \mathbf{p}^{(1)} = \frac{p^r}{\sqrt{3}} \begin{pmatrix} 1 \\ 1 \\ 1 \end{pmatrix}, \tag{5}$$

and its symmetric permutations. Each pair of variants is compatible and one can use equation (2) to calculate $\mathbf{Z}_0^S$. Carrying out the algebra, the average spontaneous strains of a single crystal span only a three-dimensional subspace of five-dimensional deviatoric strain space whereas the polarization spans the full three-dimensional polarization space. Therefore, as in the tetragonal case, $\mathbf{Z}^1$ contains only a single point in strain space unless the orientations of the grains are limited to having a common $\langle 111 \rangle_c$ axis, and it contains at least a sphere in polarization space irrespective of texture. For an equiaxed polycrystal, the spontaneous polarization of a polycrystal is $p^r/\sqrt{2}$. Further, unlike the tetragonal case, there are numerous proportions of variants that can attain any given average spontaneous strain and polarization in the set $\mathbf{Z}^S$. Thus, there is no one-to-one correlation between volume fractions and macroscopic properties.

It follows that an equiaxed rhombohedral polycrystal will not show macroscopic strains due to domain switching despite showing 70 and 109° switching and a limited ability for poling with macroscopic spontaneous polarization limited to $1/\sqrt{2}$ of the single crystal value. A polycrystal with $\langle 111 \rangle_c$ fibre-texture is necessary for macroscopic strains through 70 and 109° domain switching.

The first two predictions are consistent with the results of neutron scattering experiments on zirconium-rich (60% Zr) PZT shown in Fig. 3 as rhombohedral-SP. Note from Fig. 3a that the March coefficient of the initial specimen is less than one indicating significant electrical poling through 70 and 109° domain switching. As the sample is compressed, the March coefficient easily traverses unity, corresponding to extensive 70 and 109° domain switching. Despite this large-scale domain switching during loading, Fig. 3b shows that the strains are essentially elastic (linear). Unfortunately, the high load data are unreliable owing to the large stress involved that eventually leads to the mechanical failure of the specimen near the last data point, meaning that unloading data are unavailable. The third prediction is also consistent with observations: the single crystal spontaneous polarization value for PZN–PT is 43 μC cm$^{-2}$ and the polycrystal value is 30 μC cm$^{-2}$ in agreement with the current prediction of 30.4 μC cm$^{-2}$ (and in contrast to the classical prediction of 37.4 μC cm$^{-2}$, which does not take the compatibility between the grains into account)[4,29]. Similarly, the macroscopic strain in the polycrystal is 0.025% (ref. 29), an order of magnitude smaller than the single-crystal value of more than 1% (ref. 30). Finally, the ceramic spontaneous polarization of PZT[19] at 60% Zr is 32 μC cm$^{-2}$, and this is almost 70% of the MPB value of



©2005 Nature Publishing Group

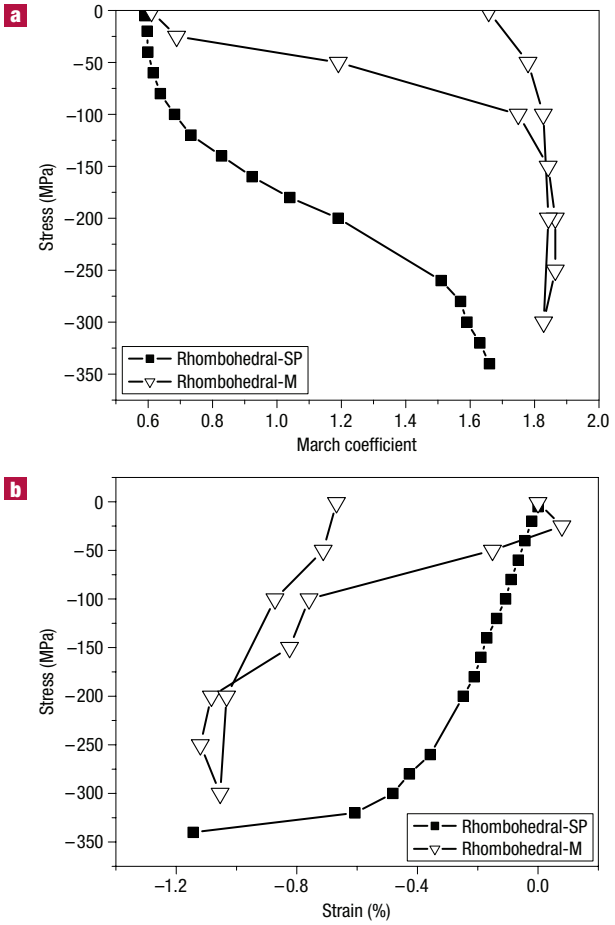


**Figure 3 The evolution under uniaxial compressive stress of the rhombodedral domains and the associated strain for two different specimens of PZT, 60/40 (rhombohedral-SP) and 49/51 (rhombohedral-M), measured *in situ* using neutron diffraction.** **a**,**b**, March coefficient (**a**) and longitudinal lattice strains (**b**) referenced to the zero-load state. Both specimens show 70 and 109° domain switching. However, this domain switching causes only linear strain in the 60/40 specimen that contains only rhombohedral domains (the nonlinearity at high loads is due to mechanical failure), but significant nonlinear strains in the morphotropic 49/51 specimen with both tetragonal and rhombohedral domains. Fitting errors are on the order of the data point symbol size and have been omitted for clarity.

48 μC cm$^{-2}$ consistent with the prediction (we show below that the MPB ceramic and single-crystal values are comparable).

### MATERIALS WITH TETRAGONAL–RHOMBOHEDRAL-PHASE CO-EXISTENCE

A material such as PZT at the MPB is cubic above the Curie temperature and can exist either as $\langle 100\rangle_c$ tetragonal or as $\langle 111\rangle_c$ rhombohedral below it (see discussion later). Thus, one has 14 variants with spontaneous strains and polarizations of the form in equations (4) and (5) and their symmetric permutations. Although the tetragonal variants are all pairwise compatible among themselves and the rhombohedral variants are all pairwise compatible among themselves, a tetragonal variant may not be compatible with a rhombohedral variant. Thus, it is not possible to apply equation (2). It is possible, however, to estimate the set $\mathbf{Z}_0^S$ from inside, and use this inner (conservative) estimate to show that $\mathbf{Z}_0^S$ spans the five-dimensional deviatoric strain space and three-dimensional polarization space. Thus, crystals with tetragonal–rhombohedral co-existence have a full dimensional set $\mathbf{Z}_0^S$. Consequently the polycrystal, irrespective of texture, has a significant set of macroscopic average strains and polarizations due to domain switching.

It follows that a polycrystal of this material would show significant amounts of 70, 90, 109 and 180° domain switching with limited inter-granular constraints, will be easy to pole and will show significant (nonlinear) macroscopic strain.

These predictions are confirmed through the neutron diffraction experiments on morphotropic PZT shown in Figs 2 and 3 as tetragonal-M and rhombohedral-M. Both of these figures contain information from the same specimen. However, as whole-pattern Rietveld analysis can be used to probe individual phases in a multiphase solid, Fig. 2 shows the March coefficient and lattice strain associated with only the tetragonal phase, whereas Fig. 3 shows those associated with only the rhombohedral phase. Note from Figs 2a and 3a that the March coefficient of the initial specimen is less than one, indicating significant domain switching during electrical poling. As the sample is compressed, the March coefficient easily traverses unity, corresponding to extensive 90, 70 and 109° domain switching. Further, this large-scale domain switching is accompanied by significant nonlinear evolution of the spontaneous strain in Figs 2b and 3b. The texture does not fully recover on unloading, and neither does the strain.

### SINGLE-PHASE MONOCLINIC MATERIALS

In a material that is cubic above the Curie temperature and monoclinic below it as reported in some PZT specimens, one has 24 variants. Not all pairs of variants are compatible in general and it is not possible to use equation (2). It is possible, however, to estimate the set $\mathbf{Z}_0^S$ from inside. Briefly, pairs of monoclinic variants that satisfy equation (1) can be combined to obtain average spontaneous strain and polarization corresponding to orthorhombic symmetry. These 12 internally laminated variants now satisfy equation (1) pairwise and yields an estimate of the set $\mathbf{Z}_0^S$ from inside. This inner estimate can be used to show that $\mathbf{Z}_0^S$ spans the five-dimensional deviatoric strain space and three-dimensional polarization space. Consequently the polycrystal, irrespective of texture, has a significant set of macroscopic average strains and polarizations. Thus, a polycrystal of this material would show significant amounts of domain switching with only limited inter-granular constraints, will be easy to pole and will show significant macroscopic strain. In other words, the effective behaviour of such a material would be very similar to that of the materials with tetragonal–rhombohedral co-existence.

## DISCUSSION

The classical view of PZT held that at the MPB composition, the $\langle 001\rangle_c$ tetragonal and $\langle 111\rangle_c$ rhombohedral phases co-exist below the Curie temperature. However, since the discovery of the monoclinic phase[16], it has been recognized a variety of phases can be found whose symmetry is contained in those of the tetragonal or rhombohedral phases. The discussion above limited itself to the traditional view because the neutron diffraction data showed an excellent fit to tetragonal and rhombohedral structures, but a poor fit to the monoclinic structure. So the specimens used in this study consisted predominantly of the tetragonal and rhombohedral structures. However, it is important to note that the main theoretical conclusions about the MPB PZT material would remain unchanged if one included the other phases: the sets $\mathbf{Z}^P$ and $\mathbf{Z}^I$ would increase slightly, but remain qualitatively unchanged.

## METHODS

Neutron diffraction is an ideal probe for bulk crystallographic structure, texture and internal strain owing to the significant penetration of neutrons. Further, a careful whole-pattern Rietveld analysis enables quantitative and simultaneous extraction of both lattice strains and domain distribution[31,32], and also the ability to probe individual phases in a multiphase material. Finally, it is insensitive to purely electrical 180° domain switching and thus isolates it from electro-mechanical domain switching.



©2005 Nature Publishing Group

Pressed, sintered ceramic samples of 40/60 tetragonal, 60/40 rhombohedral and 49/51 MPB PZT compositions were studied[31,32]. The samples were electrically poled and their diffraction pattern was recorded *in situ* at the ISIS Neutron Scattering Facility (Rutherford Appleton Laboratory, UK) while being subjected to sequentially increasing uniaxial compressive loads along the poling direction. The crystallographic data were refined using the Rietveld analysis using the GSAS software package[33].

The distribution of domains was quantified using the March–Dollase texture coefficient. In a material with a cylindrical (or fibre) texture, the probability $P_{hkl}$ of finding the ($hkl$) lattice plane depends only on the angle $\alpha$ with respect to the axis of symmetry. In the March–Dollase model, this is assumed to be proportional to the function,

$$P_{hkl}(\alpha) = \left(r^2 \cos^2\alpha + r^{-1} \sin^2\alpha\right)^{-3/2}$$

where $r$ is called the March–Dollase texture coefficient or simply the March coefficient. Thus, the entire fibre texture is described by a single coefficient $r$. This can be easily fitted to the diffraction data because the intensity of a diffraction peak is given by $I_{hkl} = P_{hkl}F_{hkl}^2$ where $F_{hkl}$ is the structure factor. The March coefficient is also impervious to 180° switching. A March coefficient of one indicates random or equiaxed texture, values less than unity indicate alignment of the polarizations along the fibre direction and values greater than unity indicate distribution of the polarizations normal to the fibre direction. Further details of the texture analysis are described elsewhere[31].

Received 7 February 2005; accepted 25 July 2005; published 18 September 2005.

## References


1. Damjanovic, D. Ferroelectric, dielectric and piezoelectric properties of ferroelectric thin films and ceramics. *Rep. Prog. Phys.* **61,** 1267–1324 (1998).
2. Cross, L. E. in *Ferroelectric Ceramics* (eds Setter, N. & Colla, E. L.) 1–85 (Birkhauser, Berlin, 1993).
3. Xu, Y. *Ferroelectric Materials and Their Applications* (North-Holland Elsevier Science, Amsterdam, 1991).
4. Jaffe, B., Cook, W. R. & Jaffe, H. *Piezoelectric Ceramics* (Academic, London, 1971).
5. Bhattacharya, K. & Ravichandran, G. Ferroelectric perovskites for electromechanical actuation. *Acta Mater.* **51,** 5941–5960 (2003).
6. Cohen, R. E. Origin of ferroelectricity in perovskite oxides. *Nature* **358,** 136–138 (1992).
7. King-Smith, R. D. & Vanderbilt, D. Theory of polarization of crystalline solids. *Phys. Rev. B* **47,** 1651–1654 (1993).
8. Resta, R. Ab initio simulation of properties of ferroelectric materials. *Mol. Simul. Mater.* **11,** R69–R96 (2003).
9. Waghmare, U. V. & Rabe, K. M. Ab initio statistical mechanics of the ferroelectric phase transition in $PbTiO_3$. *Phys. Rev. B* **55,** 6161–6173 (1997).
10. Meyer, B. & Vanderbilt, D. Ab initio study of ferroelectric domain walls in $PbTiO_3$. *Phys. Rev. B* **65,** 104111 (2002).
11. Stemmer, S., Streiffer, F. & Ruhle, M. Atomistic structure of 90 degree domain walls in ferroelectric $PbTiO_3$ thin films. *Phil. Mag. A* **71,** 713–724 (1995).
12. Shilo, D., Ravichandran, G. & Bhattacharya, K. Investigation of twin-wall structure at the nanometre scale using atomic force microscopy. *Nature Mater.* **3,** 453–457 (2004).
13. Hu, H. L. & Chen, L. Q. Three-dimensional computer simulation of ferroelectric domain formation. *J. Am. Ceram. Soc.* **81,** 492–500 (1998).
14. Ahluwalia, R. & Cao, W. W. Influence of dipolar defects on switching behavior in ferroelectrics. *Phys. Rev. B* **63,** 012103 (2001).
15. Zhang, W. & Bhattacharya, K. A computation model of ferroelectric domains. Part I. Model formulation and domain switching and Part II. Grain boundaries and defect pinning. *Acta Mater.* **53,** 185–209 (2005).
16. Noheda, D. E. *et al.* A monoclinic ferroelectric phase in $Pb(Zr_{1-x}Ti_x)O_3$. *Appl. Phys. Lett.* **74,** 2059–2061 (1999).
17. Berlincourt, D. A. & Krueger, H. A. Domain processes in lead titanate zirconate and barium titanate ceramics. *J. Appl. Phys.* **30,** 1804–1810 (1959).
18. Jaffe, B., Roth, R. S. & Marzullo, S. Piezoelectric properties of lead zirconate-lead titanate solid-solution ceramics. *J. Appl. Phys.* **25,** 809–810 (1953).
19. Berlincourt, D. A., Cmolik, C. & Jaffee, H. Piezoelectric properties of polycrystalline lead titanate zirconate compositions. *Proc. Inst. Radio Eng.* **48,** 220–229 (1960).
20. Isupov, V. A. Properties of $Pb(Ti,Zr)O_3$ piezoelectric cermaics and nature of their orientational dielectric polarization. *Sov. Phys. Solid State* **10,** 989–991 (1968).
21. Taylor, G. I. Plastic strain in metals. *J. Inst. Metals* **62,** 307–324 (1938).
22. Bhattacharya, K. & Kohn, R. V. Texture, symmetry and reoverable strains of shape-memory polycrystals. *Acta Mater.* **44,** 529–542 (1996).
23. Tickle, R., James, R. D., Shield, T., Wittig, M. & Kokorin, V. V. Ferromagnetic shape memory in the NiMnGa system. *IEEE Trans. Magn.* **35,** 4301–4310 (1999).
24. Shu, Y. C. & Bhattacharya, K. Domain patterns and macroscopic properties of ferroelectric materials. *Phil. Mag. B* **81,** 2021–2054 (2001).
25. DeSimone, A. & James, R. D. A constrained theory of magnetoelasticity. *J. Mech. Phys. Solids* **50,** 283–320 (2002).
26. Ball, J. M. & James, R. D. Fine phase mixture as minimizers of energy. *Arch. Ration. Mech. Anal.* **100,** 13–52 (1987).
27. Li, J. Y. & Liu, D. On ferroelectric crystals with engineered domain configurations. *J. Mech. Phys. Solids* **52,** 1719–1742 (2004).
28. Jona, F. & Shirane, G. *Ferroelectric Crystals* (Dover, New York, 1993).
29. Viehland, D. & Powers, J. Effect of uniaxial stress on the electromechanical properties of $0.7Pb(Mg_{1/2}Nb_{2/3})O_3$-$0.3PbTiO_3$ crystals and ceramics. *J. Appl. Phys.* **89,** 1820–1825 (2001).
30. Park, S. E. & Shrout, T. R. Ultrahigh strain and piezoelectric behavior in relaxor based ferroelectric single crystals. *J. Appl. Phys.* **82,** 1804–1811 (1997).
31. Rogan, R. C., Ustundag, E., Clausen, B. & Daymond, M. R. Texture and strain analysis of the ferroelastic behavior of $Pb(Zr,Ti)O_3$ by in situ neutron diffraction. *J. Appl. Phys.* **93,** 4104–4111 (2003).
32. Rogan, R. C. *Investigation of the Multiscale Constitutive Behavior of Ferroelectric Materials Using Advanced Diffraction Techniques.* Thesis, California Inst. Technology (2004).
33. Larson, A. C. & Von Dreele, R. B. *GSAS: General Structure Analysis System. Report No. LAUR 86-748* (Los Alamos National Laboratory, 1986).


## Acknowledgements

The authors thank M. Daymond, E. Oliver and J. Santisteban for their assistance with the experiments, a referee for suggesting the consistency check using the spontaneous polarization of PZT ceramics, and gratefully acknowledge the financial support of the US Army Research Office through DAAD 19-01-1-0517.
Correspondence and requests for materials should be addressed to K.B.
Supplementary Information accompanies this paper on www.nature.com/naturematerials.

## Competing financial interests

The authors declare that they have no competing financial interests.

Reprints and permission information is available online at http://npg.nature.com/reprintsandpermissions/



©2005 Nature Publishing Group